Effect of CO_2 dilution with Methane in Thermal Pulse Combustor

Sirshendu Mondal*[1], Achintya Mukhopadhyay[2], Swarnendu Sen[1]

[1] Mechanical Engineering Department, Jadavpur University
188, Raja S. C. Mullick Rd, Jadavpur, Kolkata, 700032, India
[2] Mechanical Engineering Department, IIT Madras
S. P. Road, Kanagam, Chennai, 600036, India
* Corresponding author: sirshosona@gmail.com

Pulse combustors, one type of air-breathing engines in which combustion takes place through a series of discrete event, are applied for heating, drying and even propulsion applications. However, fundamentals of this pulse combustor remain till date largely unexplored. For this present study, the experiments are carried out using CH_4 and CH_4 - CO_2 blend as fuel in a Helmholtz-type, non-premixed, valveless pulse combustor. It is found from the FFT analysis of the pressure data of methane flame, the frequencies have no such dependence on equivalence ratio though it has strong dependence on overall flow rate because the higher turbulence with higher flow rate reduces the ignition delay time. From frequency and amplitude analysis of CH_4 - CO_2 flame, the hysteresis loop is clearly seen in terms of both frequency and amplitude with the variation of % of CO_2 dilution which suggests the possibility of causing a transition from the high amplitude limit cycle to the low amplitude limit cycle.

1 Introduction

Pulse Combustors are a class of air-breathing engines in which pulsations in combustion are utilized to improve the performance. Pulse combustors provide several advantages over their steady flow counterparts like lower emission, higher rates of convective heat transfer in the tailpipe and higher thermal efficiency. These advantages have been exploited in different designs of pulse combustors mainly for heating and drying applications. Pulse combustors also have potential for propulsion applications, particularly for micro-propulsion vehicles. In addition, Depending on the presence of mechanical valves at the inlet, such combustors are classified as valved or valveless. In valveless combustors, self-sustained combustion oscillations are obtained even with steady inflow of reactants. In spite of the advantages offered by pulse combustors, their applications have been rather limited because of the lack of understanding of the complex dynamics of the process.

Richards et al. [1] developed a model of thermal pulse combustor that produces oscillatory combustion even with steady inflow of reactants. They used unsteady well-stirred reactor models and coupled it a lumped model for gas flow in the tailpipe. Their results showed pulsating combustion in the intermediate ranges of operating parameters. Daw et al. [2] developed a mathematical model based on the work of Richards et al. [1] and also carried out experiments on a laboratory-scale combustor to demonstrate the existence of bifurcations in the combustor performance that ultimately led to chaos. Rhode et al. [3] used the model of Richards et al. [1] to demonstrate that the flammable range of flow time can be extended by controlling the chaos using friction factor as the control variable. Mukhopadhyay et al. [4], Datta et al. [5] and Mondal et al. [6] investigated the effects of different parameters on the nonlinear dynamics and possible transition to chaos in pulse

combustors using the model of Richards et al. [1]. Gupta et al. [7], Datta et al. [8] and Chakraborty et al. [9] applied the tools of symbolic dynamics to the above model of pulse combustors to predict extinction in pulse combustors. Xu et al. [10] analyzed the effect of different parameter on combustion stability both theoretically and experimentally. Margolis [11] analysed the nonlinear dynamics of a Helmholtz-type pulse combustor and showed that the nonlinear acoustic oscillations arise from the combustion-driven instabilities exciting the acoustic modes. Tang et al. [12] showed the oscillations in a pulse combustor to be a consequence of coupling of several acoustic and hydrodynamic factors. Bloom et al. [13–15] studied the nonlinear dynamics of pulse combustor but focused their study on valved pulse combustors. Jones et al. [16] showed the effect of fuel composition on the operational characteristics of commercially available non-premixed pulse combustor adding H_2 and C_3H_8 with CH_4 separately. They presented the variation in amplitude and frequency of pressure oscillation due to the change in ignition delay time for different fuel composition. Kushari et al. [17] investigated the fuel effect on the performance of pulse combustors by comparing the amplitude and phase of oscillations for pulse combustors using CH_4 and CH_4 - H_2 mixture as fuel diluted with CO_2 and He to vary the heat content. They used a Helmholtz-type, non-premixed, valved pulse combustor. Zhonghua and Mujumdar [18] numerically investigated pulsed combustion of different fuels but focused mainly on liquid bio-fuels.

The objective of the present work is to conduct a more comprehensive investigation of the acoustic bahaviour in terms of the frequency and amplitude of pressure pulsations of a thermal pulse combustor using the CH_4 and CH_4-CO_2 blend as fuel. The motivation behind choosing these fuel is that the former is a surrogate of a common industrial fuel, natural gas and the CH_4 - CO_2 blend closely simulates landfill gas. Furthermore, the flue gas recirculation, which can suppress NO_X emission and improve heat transfer in combustion chambers, is an important technique in industrial applications and CO_2 is the main species in the flue gas. In section 2, a description of experimental set-up and instrumentation is given with a scematic diagram. In section 3, results are presented with explanation which consists of two subsection, one for pure CH_4 and other for CH_4-CO_2 blend. Section 4 and 5 are committed for conclusion and acknowledgment respectively.

2 Experimental Setup

The set-up (shown in Fig. 1) consists of an upstream section, the combustor and the tailpipe. All metal parts are made of SS316 stainless steel that withstands high temperatures. The combustor is designed to provide optically accessible flames. It consists of a 200 mm long quartz tube of inner diameter 60 mm and outer diameter 65 mm to allow optical access. The quartz tube is held between two grooved flanges by two long rods threaded to the flanges. At the base of the combustor and near the top, provisions are made for mounting pressure transducers and spark plug for ignition. The lower flange of the combustor is fastened to the flange of the inlet section with 6 bolts. Fuel is admitted through 2 mm diameter holes drilled in two rows 180° apart on a 6 mm diameter hollow steel pipe that spanned almost the entire diameter of the combustor. Fuel is injected horizontally at cross flow with the air stream. Air is admitted axially at the bottom of the upstream section. The tailpipe consists of two pipes of diameter 25 mm and length 300 mm each, flanged at the ends. The tailpipe is open to the atmosphere. The tailpipe length can be varied by using one or both pipes. For the present study both tail pipes are used. The direct exposure of pressure transducer to hot combustible gases may hamper the diaphragm of piezoelectric pressure transducer. For acquiring the dynamic pressure from the combustor, a cooling jacket is designed and fastened to the combustion chamber to cool the piezoelectric diaphragm. The fuel (CH_4 and CH_4 - CO_2 blend) is supplied from a pressurized cylinder while air is supplied by means of a compressor through a pressure regulator (by means of which upstream pressure is maintained at 3 bars). Fuel and air flow rates are measured with high precision mass flow controllers of Aalborg make. The mass flow controller for air has a maximum flow rate of 500 lpm while that for CH_4 and CO_2 has a maximum flow rate of 60 lpm and 100 lpm respectively. The pressure inside the combustion chamber is measured with a piezoelectric dynamic pressure transducer of Kistler make. The output of the pressure transducer is fed to National Instruments PXI data acquisition

system through an amplifier which converts the charge generated by the piezoelectric sensor to the voltage. Data is acquired for this sensor at a sampling rate of 2000 Hz for 20 seconds. Such a high frequency of sampling is set so that no frequency of dynamics is missed up to 1000 Hz (Nyquist criterion). A digital filter is used to remove the AC frequency noise ($\sim$ 50 Hz and its harmonics) from pressure transducer data. In the post processing stage the sampling frequency is reduced by simply skipping intermediate data depending upon the frequency range of combustion. The time series voltage data recorded by the pressure transducer are then processed to generate the amplitude spectrum.

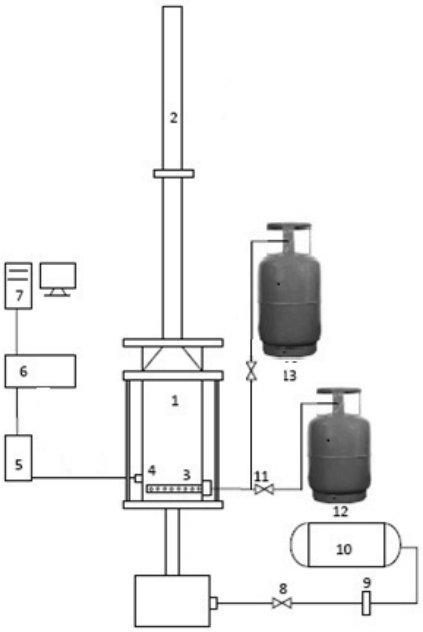

Figure 1: Schematic of the experimental set-up. (1) Combustor, (2) Tailpipe, (3) Fuel inlet, (4) Pressure Transducer, (5) Dynamic amplifier, (6) Data acquisition system, (7) PC, (8) Control valve for air line, (9) Pressure Regulator, (10) Compressor, (11) Control valve for fuel line, (12) CH_4 cylinder, (13) CO_2 cylinder

CH_4 and CH_4 - CO_2 blend are used as fuel. In a particular experiment, air flow is kept fixed while fuel flow is progressively reduced to maintain a global equivalence ratio roughly between 1.1 and 0.5. This ensures that the mixture flow rate is nearly constant (as the A/F ratio for CH_4 is 17.16) to keep the flow time almost unchanged. Thus the differences in observed phenomena are caused primarily by the difference in heat release rates. Air flow rate is also varied from 80 lpm to 160 lpm. By varying the air flow rate and/or introducing CO_2, the change in the aerodynamics is also taken into account.

3 Results and Discussion

To examine the effect of fuel on dynamics of pulse combustors, experiments are carried out using CH_4, CH_4 - CO_2 blend. The former is a surrogate of a common industrial fuel, natural gas. On the other hand, the CH_4 - CO_2 blend closely simulates landfill gas.

3.1 CH_4 as fuel

Using methane, the experimentation is conducted with 5 different air flow rate i.e. 80, 100, 120, 140, 160 lpm. For each air flow rate the equivalence ratio (ϕ) of methane is varied and the time series data of pressure has been captured. Then Fast Fourier Transform (FFT) is computed on the time series data to examine the existence of any dominant frequency of oscillation.

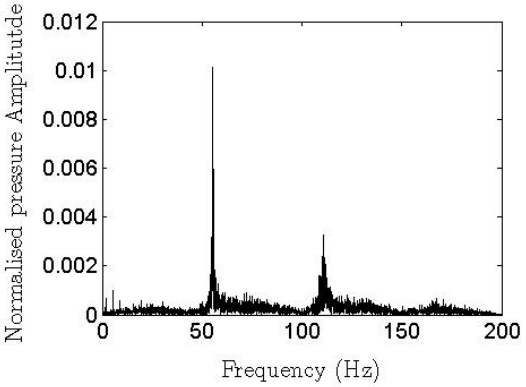

Figure 2: FFT plots of $\phi = 0.73$, keeping the air flow rate at 100 lpm

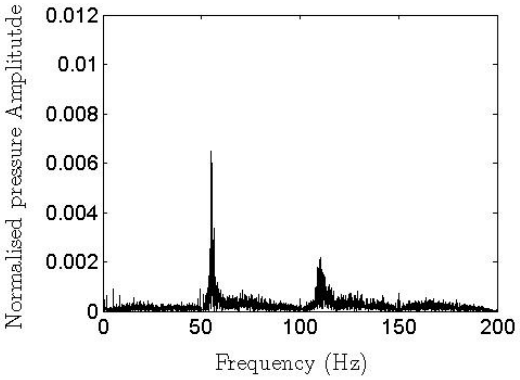

Figure 3: FFT plots of $\phi = 0.99$, keeping the air flow rate at 100 lpm

In figure 2 and 3, the FFT plots for $\phi = 0.73$ and 0.99 of methane with 100 lpm air flow rate are shown. In figures, two different sharp peaks are seen which presents in the FFT plots of all other equivalence ratios. From the magnitude of frequencies, it is clear that the second dominant frequency is the harmonic of first one. For investigating the dependence of dominant frequencies on ϕ and air flow rate, frequencies (1st harmonic) have been plotted against ϕ for different air flow rates in figure 4.

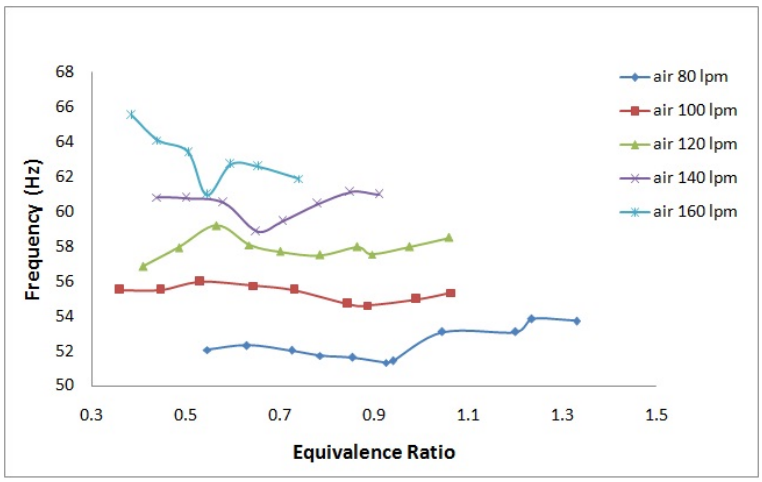

Figure 4: Dependence of pulsating frequencies on ϕ

It is clear from the figure that frequencies have no clear dependence on ϕ as the curves are more or less parallel with the horizontal axis specially for low flow rates. But it has a strong dependence on air flow rate. Frequencies increases with the increase of air flow rate because the higher turbulence with higher flow rate reduces the ignition delay time. Both of the dominant frequencies show the same trend with the variation of flow rate. The total ignition delay time in

pulse combustor is contributed by three different process: (1) $\tau_{species}$, the time required for air and fuel to mix, (2) τ_{mixing}, the time required for the incoming reactants to mix with the ignition source in the form of "hot products" remaining from the previous cycle, and (3) $\tau_{kinetic}$, the post mixing chemical ignition time [17,19]. The total ignition delay time, $\tau_{ignition}$, is then given by

$$\tau_{ignition} = f(\tau_{species}, \tau_{mixing}, \tau_{kinetic}) \tag{1}$$

For a given fuel (CH_4), $\tau_{kinetic}$ remains fixed whereas the $\tau_{species}$ and τ_{mixing} decrease due to the increase in turbulence. The pulsating frequency increases with the reduction of ignition delay time [16] which is clear from figure 4.

3.2 CH_4 - CO_2 blend as fuel

For CH_4 - CO_2 blend, the % of CO_2 dilution(in terms of volume flow rate) is varied keeping air and methane flow rate constant. This is done this way to investigate the effect of dilution for a particular equivalence ratio of CH_4. In this mixture, CH_4 acts as a fuel whereas CO_2 being an inert gas only dilutes the mixture.

In figure 5, the FFT plots and time-series of pressure fluctuation for 0%, 20% and 40% dilution of CO_2 with CH_4 are presented where air flow rate is kept fixed at 100 lpm and $\phi = 1$. The frequency and amplitude of pressure fluctuation in the case of 20% dilution is quite similar to that in the case of pure CH_4 which is very clear from the last two columns of the figure below.

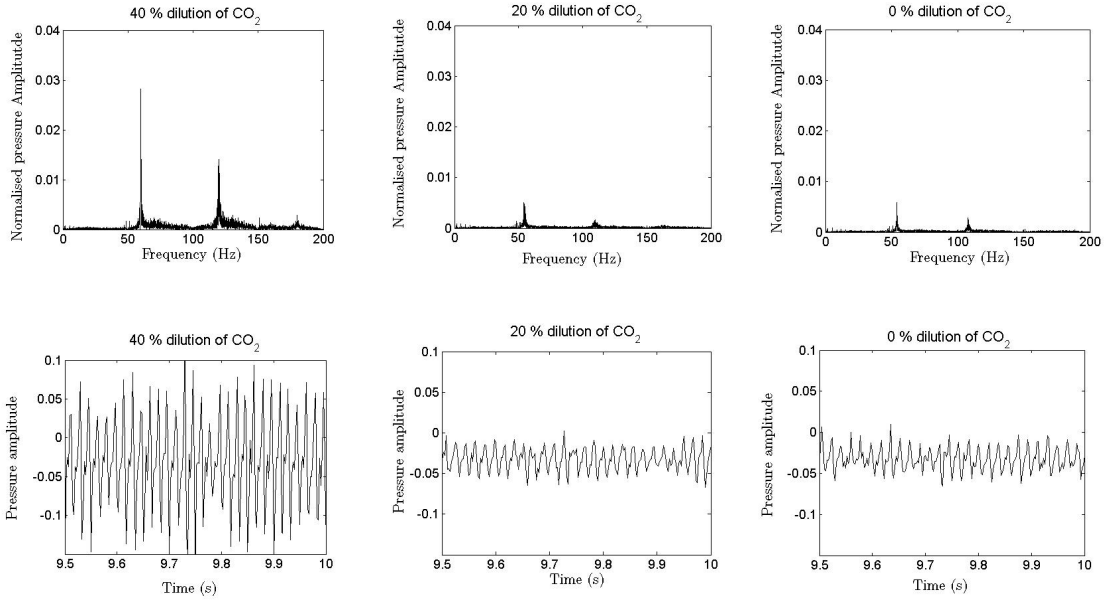

Figure 5: FFT and time-series plots for different % dilution of CO_2 with CH_4 keeping air flow at 100 lpm and $\phi = 1$

But in case of higher dilution of CO_2, frequency increases slightly whereas the increase of amplitude is remarkable. As CO_2 being a inert gas, it has only the effect on aerodynamics of the flow. The higher dilution increases the overall flow rate which in turn reduces the $\tau_{species}$ and τ_{mixing}. But, on the other hand, CO_2 dilution causes to decrease the laminar burning speed [20] of CH_4, which eventually increases the $\tau_{kinetic}$. In overall effect, the frequency of pressure oscillations slightly increases due to the overall decrease of $\tau_{ignition}$. The growth in amplitude of acoustic oscillation indicates that the periodic heat release is in phase with the pressure oscillation and drives the oscillations as stated by the Rayleigh criterion which can be stated by following equation.

$$P.Q.\cos(\theta) = L \tag{2}$$

where P and Q are the pressure and heat release amplitudes, θ is the phase angle between them, and L is the sum of all losses during the cycle. Thus, if θ is less than 90°, the heat addition process will drive the pressure oscillations, otherwise it will damp.

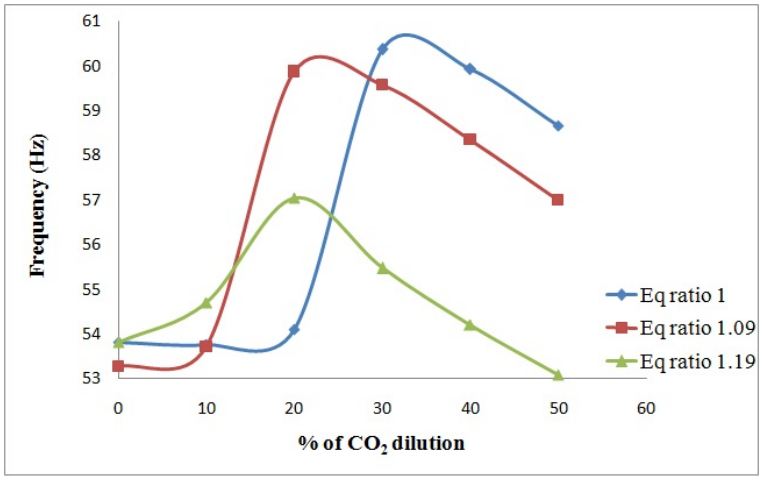

Figure 6: Dependence of % of dilution on frequencies for different equivalence ratios, keeping air flow rate fixed at 100 lpm

The left-hand side of equation 2 represent the driving of the pressure pulsations by the heat release fluctuations. When this driving is balanced by the acoustic losses, represented by the right-hand side of the equation, the pulse combustor operates in its limit cycle. If the magnitude of the heat release oscillations is increased, the driving process becomes stronger, causing an increase in acoustic pressure amplitudes. At the same time, the acoustic losses increase with increasing acoustic pressure amplitudes until the system operates in a new limit cycle with higher sound pressure level. With higher dilution of CO_2, magnitude of the heat release oscillations is increased due to higher turbulence (as better mixing intensify the combustion) resulting from increased overall flow rate. So, with increase of CO_2 dilution, a new limit cycle with higher amplitude is formed which is clearly visible in figure 5.

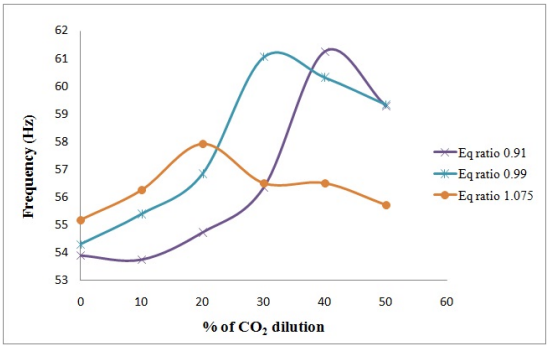

Figure 7: Dependence of % of dilution on frequencies for different equivalence ratios, keeping air flow rate fixed at 120 lpm

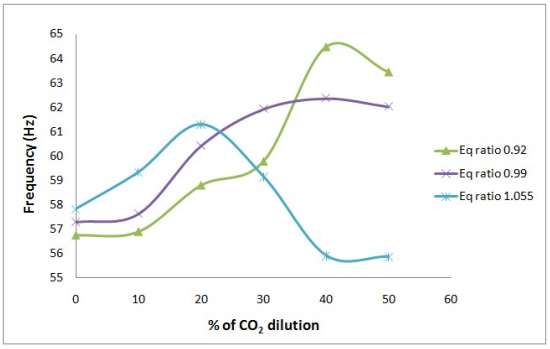

Figure 8: Dependence of % of dilution on frequencies for different equivalence ratios, keeping air flow rate fixed at 140 lpm

In figure 6, effect of dilution on frequencies has been plotted for different equivalence ratios,

keeping air flow rate fixed at 100 lpm. Here, only first dominant frequencies have been plotted. It is clear from the figure that, with the increase of CO_2, frequency suddenly jumps to a higher value and then decreases for each equivalence ratio. Initially, the frequency increases due to the reduction of ignition delay time (as $\tau_{species}$ and τ_{mixing} decrease due to the increased turbulence) but with the addition of more CO_2, the increase of $\tau_{kinetic}$ (due to reduced laminar burning speed) predominates and the frequency decreases slightly.

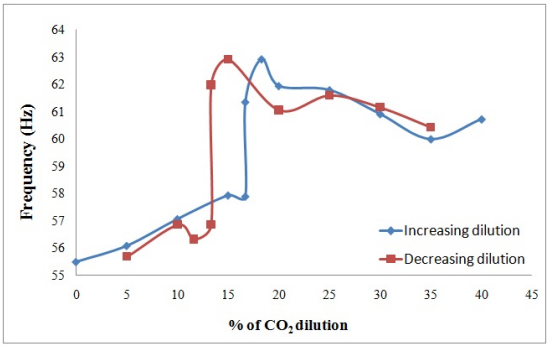

Figure 9: Hysteresis loop in terms of frequency

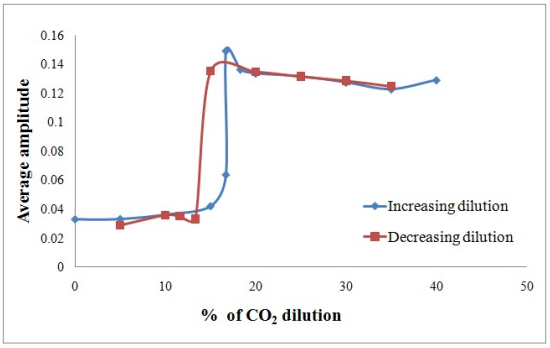

Figure 10: Hysteresis loop in terms of average amplitude

Moreover, this increase of frequency is higher in lower equivalence ratio. For higher equivalence ratio, more fuel is introduced in the combustion chamber and the time required for air and fuel to mix is increased nevertheless the overall flow rate slightly increases. In effect, $\tau_{species}$ increases which in turn decreases the frequency. This study has also been carried out with air flow rate 120 lpm and 140 lpm. The variations of frequency with % of CO_2 dilution for higher air flow rates are presented in figure 7 and 8.

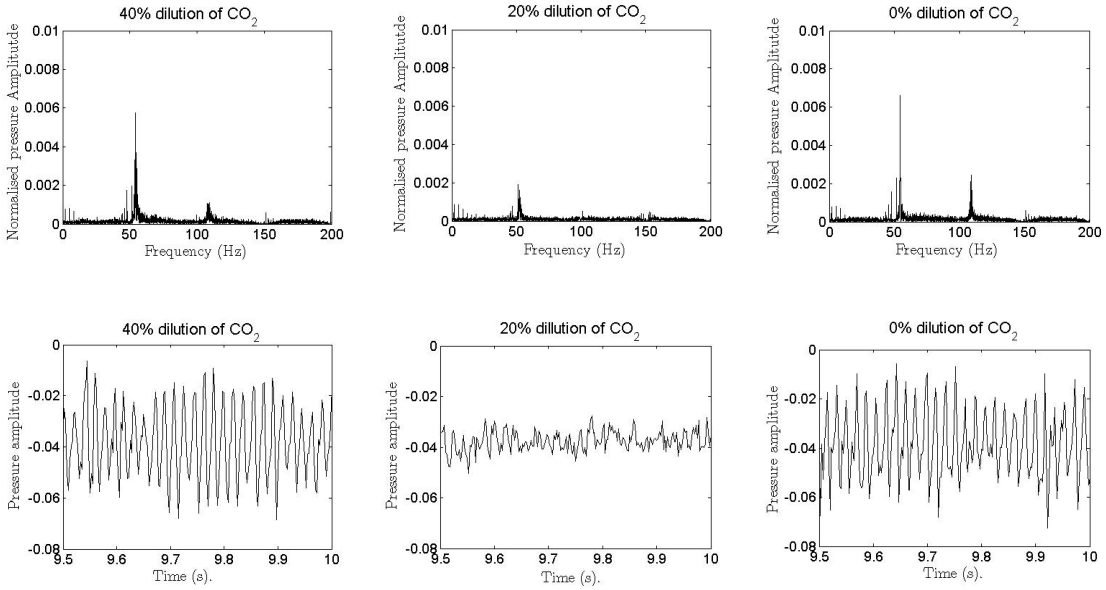

Figure 11: FFT and time-series plots for different % dilution of CO_2 with CH_4 keeping air flow at 120 lpm and $\phi = 0.83$

Similar trends are found for higher flow rate. As the reactant flow rate becomes higher, the ignition delay time ($\tau_{species}$ and τ_{mixing} to be specific) decreases due to higher turbulence. As a

result of that the frequencies in the case of 120 lpm and 140 lpm increase slightly compare to the case of 100 lpm.

For a certain percentage of CO_2 a higher frequency and higher amplitude oscillation starts and in reverse way it goes off in the different value of CO_2 percentage. A hysteresis loop is found in terms of both frequency and average amplitude. The later is calculated by averaging the differences between consecutive upper and lower peaks in the time series data. The hysteresis loop is presented in terms of both frequency and average amplitude in figure 9 and 10 respectively for air flow rate 120 lpm and $\phi = 0.99$. The upper branch represents relatively high amplitude limit cycles and the lower branch contains low level oscillations. Existence of the hysteresis loop suggests the possibility of causing a transition from the upper unstable branch to the lower stable branch [21]. This sort of hysteresis considered here is associated with a subcritical bifurcation (producing the instability at 15 % of CO_2 dilution).

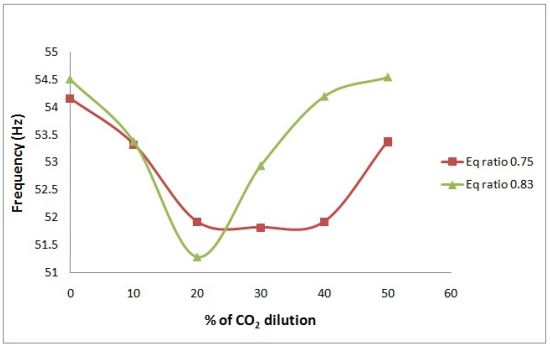

Figure 12: Dependence of % of dilution on frequencies for different low equivalence ratios, keeping air flow rate fixed at 120 lpm

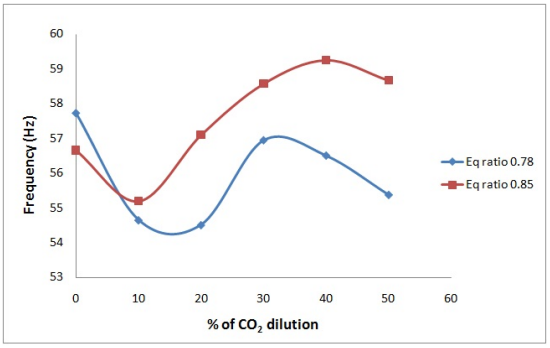

Figure 13: Dependence of % of dilution on frequencies for different low equivalence ratios, keeping air flow rate fixed at 140 lpm

So far, the results are presented are for near stoichiometric equivalence ratio. Using comparatively lean mixture, a different pattern of frequency and amplitude of pressure oscillation with the variation of CO_2 dilution is found. In figure 11, the FFT plots and time-series of pressure fluctuation for 0%, 20% and 40% dilution of CO_2 with CH_4 are presented where air flow rate is kept fixed at 120 lpm and $\phi = 0.83$. It is clear from figure that both frequency and amplitude decrease first and then increase with the increase of CO_2. Initially overall ignition delay is predominated by $\tau_{kinetic}$ which increases due to the decrease of laminar burning speed and the frequency and amplitude starts decreasing. But, with more introduction of CO_2, $\tau_{species}$ and τ_{mixing} decrease due to the higher turbulence, and the decrease of overall ignition delay causes to increases the frequency and amplitude. This sort of variation in frequency and amplitude for lower equivalence ratio is also found for different air flow rates which are shown in figure 12 and 13 for air flow rate 120 lpm and 140 lpm respectively. The opposite trend in frequency and amplitude which is found for lower equivalence ratios is due to two factors: (1) with the decrease of equivalence ratio the overall flow rate slightly decreases which increases $\tau_{species}$ and τ_{mixing}, (2) the average temperature in the combustion chamber, which decreases with the decrease of equivalence ratio, causes to increase the $\tau_{kinetic}$ [17]. So, for lower equivalence ratio, the overall ignition delay time is higher than that for the higher equivalence ratio.

4 Conclusion

Effect of CO_2 dilution with Methane was investigated using a laboratory scale thermal pulse combustor with different flow rates. For each flow rate the equivalence ratios has been varied. The air was admitted axially through the base of the combustor. Fuel was admitted through

holes drilled on a pipe that spanned the base of the combustor. The pressure is measured with a piezoelectric pressure transducer. A digital filter is used to remove the AC frequency noise ($\sim$ 50 Hz and its harmonics) from pressure transducer data. The experiments are carried out using CH_4, CH_4 - CO_2 blend to simulate the natural gas and landfill gas respectively. For the case of pure CH_4, frequencies have no clear dependence on ϕ but it has a strong dependence on air flow rate. Frequencies increases with the increase of air flow rate because the higher turbulence with higher flow rate reduces the ignition delay time. In case of higher dilution of CO_2, frequency increases slightly whereas the increase of amplitude is remarkable. With higher dilution of CO_2, magnitude of the heat release oscillations is increased due to higher turbulence resulting from increased overall flow rate. So, with increase of CO_2 dilution, a new limit cycle with higher amplitude is formed. With the increase of CO_2, frequency suddenly jumps to a higher value and then decreases as with the addition of more CO_2, $\tau_{kinetic}$ increases resulting from the reduction of laminar burning speed and the frequency decreases slightly. Similar trend has also been found for higher air flow rates. A hysteresis loop is found in terms of both frequency and average amplitude with the variation of % of CO_2 dilution which suggests the possibility of causing a transition from the upper unstable branch to the lower stable branch. The opposite trend in frequency and amplitude is found for lean equivalence ratios.

5 Acknowledgment

This work has been supported by Council of Scientific and Industrial Research (CSIR), Government of India. The first author gratefully acknowledges the Senior Research Fellowship from CSIR.

References

[1] G. A. Richards, G. J. Morris, D. W. Shaw, S. A. Keeley, and M. J. Welter. Thermal pulse combustion. *Combustion Science and Technology*, 94(1-6):57–85, 1993.

[2] C. S. Daw, J. F. Thomas, G. A. Richards, and L. L. Narayanaswami. Chaos in thermal pulse combustion. *Chaos*, 5(4):662–670, 1995.

[3] M. A. Rhode, R. W. Rollins, A.J. Markworth, K. D. Edwards, K. Nguyen, C. S. Daw, and J. F. Thomas. Controlling chaos in a model of thermal pulse combustion. *Journal of Applied Physics*, 78(4):2224–2232, 1995.

[4] A. Mukhopadhyay, S. Datta, and D. Sanyal. Effects of tailpipe friction on the nonlinear dynamics of a thermal pulse combustor. *Transactions of ASME Journal of Engineering for Gas Turbines and Power*, 130(1):011507(1) – 011507(9), 2008.

[5] S. Datta, S. Mondal, A. Mukhopadhyay, D. Sanyal, and S. Sen. An investigation of nonlinear dynamics of a thermal pulse combustor. *Combustion Theory and Modelling*, 13(1):17–38, 2009.

[6] S. Mondal, A. Mukhopadhyay, and S. Sen. Effects of inlet conditions on dynamics of a thermal pulse combustor. *Combustion Theory and Modelling*, 16(1):59–74, 2012.

[7] S. Gupta, A. Ray, and A. Mukhopadhyay. Anomaly detection in thermal pulse combustors using symbolic time series analysis. *Proceedings of the Institution of Mechanical Engineers, Part I: Journal of Systems and Control Engineering*, 220(5):339–351, 2006.

[8] S. Datta, A. Mukhopadhyay, and D. Sanyal. Use of temporal irreversibility of symbolic time series for early detection of extinction in thermal pulse combustors. In *ASME 2006 International Mechanical Engineering Congress and Exposition*, pages 127–135, Chicago, USA, November, 5 – 10, 2006.

[9] S. Chakraborty, S. Gupta, A. Ray, and A. Mukhopadhyay. Data-driven fault detection and estimation in thermal pulse combustors. *Proceedings of the Institution of Mechanical Engineers, Part G: Journal of Aerospace Engineering*, 222(8):1097–1108, 2008.

[10] Y. Xu, M. Zhai, P. Dong, F. Wang, and Q. Zhu. Modeling of a self-excited pulse combustor and stability analysis. *Combustion Theory and Modelling*, 15(5):623–643, 2011.

[11] S. B. Margolis. The nonlinear dynamics of intrinsic acoustic oscillations in a model pulse combustor. *Combustion and Flame*, 99(2):311 – 322, 1994.

[12] Y.M. Tang, G. Waldherr, J.I. Jagoda, and B.T. Zinn. Heat release timing in a nonpremixed helmholtz pulse combustor. *Combustion and Flame*, 100(1–2):251 – 261, 1995.

[13] F. Bloom, F. Ahrens, and T. Patterson. The nonlinear dynamical system generated by the AKT pulse combustor model. *Nonlinear Analysis: Theory, Methods and Applications*, 63(5–7):891 – 901, 2005.

[14] F. Bloom and T. Patterson. The effect of tailpipe friction on pressure and velocity oscillations in a nonlinear, lumped parameter, pulse combustor model. *Nonlinear Analysis: Real World Applications*, 10(5):3002 – 3017, 2009.

[15] F. Bloom, O. Terlyga, and T. Patterson. Perturbation analysis of self-sustained oscillations in a pulse combustion model. *Nonlinear Analysis: Real World Applications*, 11(4):2314 – 2334, 2010.

[16] H.R.N. Jones and J. Leng. The effect of hydrogen and propane addition on the operation of a natural gas-fired pulsed combustor. *Combustion and Flame*, 99(2):404 – 412, 1994.

[17] A. Kushari, L.J. Rosen, J.I. Jagoda, and B.T. inn. The effect of heat content and composition of fuel on pulse combustor performance. *Symposium (International) on Combustion*, 26(2):3363 – 3368, 1996.

[18] W. Zhonghua and A. S. Mujumdar. Pulse combustion characteristics of various gaseous fuels. *Energy & Fuels*, 22(2):915–924, 2008.

[19] J.O. Keller, T.T. Bramlette, J.E. Dec, and C.K. Westbrook. Pulse combustion: The importance of characteristic times. *Combustion and Flame*, 75(1):33 – 44, 1989.

[20] F. Halter, F. Foucher, L. Landry, and C. Mounaïm-Rousselle. Effect of dilution by nitrogen and/or carbon dioxide on methane and iso-octane air flames. *Combustion Science and Technology*, 181(6):813–827, 2009.

[21] P. Knoop, F.E.C. Culick, and E.E. Zukoski. Extension of the stability of motions in a combustion chamber by nonlinear active control based on hysteresis. *Combustion Science and Technology*, 123(1-6):363–376, 1997.